AXIONS AND OTHER SIMILAR PARTICLES

Revised January 2010 by C. Hagmann (LLNL), H. Murayama (UC Berkeley), G.G. Raffelt (MPI Physics), L.J. Rosenberg (U. of Washington), and K. van Bibber (LLNL).

Introduction

In this section, we list coupling-strength and mass limits for light neutral scalar or pseudoscalar bosons that couple weakly to normal matter and radiation. Such bosons may arise from a global spontaneously broken U(1) symmetry, resulting in a massless Nambu-Goldstone (NG) boson. If there is a small explicit symmetry breaking, either already in the Lagrangian or due to quantum effects such as anomalies, the boson acquires a mass and is called a pseudo-NG boson. Typical examples are axions (A^0) [1,2], familons [3] and Majorons [4], associated, respectively, with a spontaneously broken Peccei-Quinn, family and lepton-number symmetry.

A common characteristic among these light bosons ϕ is that their coupling to Standard-Model particles is suppressed by the energy scale that characterizes the symmetry breaking, $i.e.$, the decay constant f. The interaction Lagrangian is

$$\mathcal{L} = f^{-1} J^\mu \partial_\mu \phi \,, \tag{1}$$

where J^μ is the Noether current of the spontaneously broken global symmetry. If f is very large, these new particles interact very weakly. Detecting them would provide a window to physics far beyond what can be probed at accelerators.

Axions remain of particular interest because the Peccei-Quinn (PQ) mechanism remains perhaps the most credible scheme to preserve CP in QCD. Moreover, the cold dark matter of the universe may well consist of axions and they are searched for in dedicated experiments with a realistic chance of discovery.

Originally it was assumed that the PQ scale f_A was related to the electroweak symmetry-breaking scale $v_{\mathrm{weak}} = (\sqrt{2}G_{\mathrm{F}})^{-1/2} = 247$ GeV. However, the associated "standard" and "variant" axions were quickly excluded—we refer to the Listings for detailed limits. Here we focus on "invisible axions" with $f_A \gg v_{\mathrm{weak}}$ as the main possibility.

Axions have a characteristic two-photon vertex, inherited from their mixing with π^0 and η. It allows for the main search strategy based on axion-photon conversion in external magnetic fields [5], an effect that also can be of astrophysical interest. While for axions the product "$A\gamma\gamma$ interaction strength × mass" is essentially fixed by the corresponding π^0 properties, one may consider more general axion-like particles (ALPs) where the two parameters are independent. Several experiments have recently explored this more general parameter space.

I. THEORY

I.1 Peccei-Quinn mechanism and axions

The QCD Lagrangian includes a CP-violating term $\mathcal{L}_\Theta = \bar\Theta\,(\alpha_s/8\pi)\,G^{\mu\nu a}\tilde{G}^a_{\mu\nu}$, where $-\pi \leq \bar\Theta \leq +\pi$ is the effective Θ parameter after diagonalizing quark masses, G is the color field strength tensor, and $\tilde{G}$ its dual. Limits on the neutron electric dipole moment [6] imply $|\bar\Theta| \lesssim 10^{-10}$ even though $\bar\Theta = \mathcal{O}(1)$ is otherwise completely satisfactory. The spontaneously broken global Peccei-Quinn symmetry $U(1)_{PQ}$ was introduced to solve this "strong CP problem" [1], an axion being the pseudo-NG boson of $U(1)_{PQ}$ [2]. This symmetry is broken due to the axion's anomalous triangle coupling to gluons,

$$\mathcal{L} = \left(\bar\Theta - \frac{\phi_A}{f_A}\right)\frac{\alpha_s}{8\pi}\,G^{\mu\nu a}\tilde{G}^a_{\mu\nu}\,, \qquad (2)$$

where ϕ_A is the axion field and f_A the axion decay constant. Color anomaly factors have been absorbed in the normalization of f_A which is defined by this Lagrangian. Thus normalized, f_A is the quantity that enters all low-energy phenomena [7]. Non-perturbative effects induce a potential for ϕ_A whose minimum is at $\phi_A = \bar\Theta\,f_A$, thereby canceling the $\bar\Theta$ term in the QCD Lagrangian and thus restoring CP symmetry.

The resulting axion mass is given by $m_A f_A \approx m_\pi f_\pi$ where $m_\pi = 135$ MeV and $f_\pi \approx 92$ MeV. In more detail one finds

$$m_A = \frac{z^{1/2}}{1+z}\frac{f_\pi m_\pi}{f_A} = \frac{0.60\ \text{meV}}{f_A/10^{10}\,\text{GeV}}\,, \qquad (3)$$

where $z = m_u/m_d$. We have used the canonical value $z = 0.56$ [8], although the range $z = 0.35$–0.60 is plausible [9].

Originally one assumed $f_A \sim v_{\text{weak}}$ [1,2]. Tree-level flavor conservation fixes the axion properties in terms of a single parameter $\tan\beta$, the ratio of the vacuum expectation values of two Higgs fields that appear as a minimal ingredient. This "standard axion" is excluded after extensive searches [10]. A narrow peak structure observed in positron spectra from heavy ion collisions [11] suggested an axion-like particle of mass 1.8 MeV that decays into e^+e^-, but extensive follow-up searches were negative. "Variant axion models" were proposed which keep $f_A \sim v_{\text{weak}}$ while dropping the constraint of tree-level flavor conservation [12], but these models are also excluded [13].

Axions with $f_A \gg v_{\text{weak}}$ evade all current experimental limits. One generic class of models invokes "hadronic axions" where new heavy quarks carry U(1)_{PQ} charges, leaving ordinary quarks and leptons without tree-level axion couplings. The prototype is the KSVZ model [14], where in addition the heavy quarks are electrically neutral. Another generic class requires at least two Higgs doublets and ordinary quarks and leptons carry PQ charges, the prototype being the DFSZ model [15]. All of these models contain at least one electroweak singlet scalar that acquires a vacuum expectation value and thereby breaks the PQ symmetry. The KSVZ and DFSZ models are frequently used as generic examples, but other models exist where both heavy quarks and Higgs doublets carry PQ charges.

I.2 Model-dependent axion couplings

Although the generic axion interactions scale approximately with f_π/f_A from the corresponding π^0 couplings, there are non-negligible model-dependent factors and uncertainties. The axion's two-photon interaction plays a key role for many searches,

$$\mathcal{L}_{A\gamma\gamma} = \frac{G_{A\gamma\gamma}}{4} F_{\mu\nu}\tilde{F}^{\mu\nu}\phi_A = -G_{A\gamma\gamma}\mathbf{E}\cdot\mathbf{B}\,\phi_A\,, \qquad (4)$$

where F is the electromagnetic field-strength tensor and $\tilde{F}$ its dual. The coupling constant is

$$\begin{aligned}
G_{A\gamma\gamma} &= \frac{\alpha}{2\pi f_A}\left(\frac{E}{N} - \frac{2}{3}\frac{4+z}{1+z}\right) \\
&= \frac{\alpha}{2\pi}\left(\frac{E}{N} - \frac{2}{3}\frac{4+z}{1+z}\right)\frac{1+z}{z^{1/2}}\frac{m_A}{m_\pi f_\pi}\,,
\end{aligned} \qquad (5)$$

where E and N are the electromagnetic and color anomalies of the axial current associated with the axion. In grand unified models, and notably for DFSZ [15], $E/N = 8/3$, whereas for KSVZ [14] $E/N = 0$ if the electric charge of the new heavy quark is taken to vanish. In general, a broad range of E/N values is possible [16]. The two-photon decay width is

$$\Gamma_{A\to\gamma\gamma} = \frac{G_{A\gamma\gamma}^2 m_A^3}{64\,\pi} = 1.1 \times 10^{-24}\ \text{s}^{-1}\left(\frac{m_A}{\text{eV}}\right)^5. \qquad (6)$$

The second expression uses Eq. (5) with $z = 0.56$ and $E/N = 0$. Axions decay faster than the age of the universe if $m_A \gtrsim 20$ eV.

The interaction with fermions f has derivative form and is invariant under a shift $\phi_A \to \phi_A + \phi_0$ as behooves a NG boson,

$$\mathcal{L}_{Aff} = \frac{C_f}{2f_A}\,\bar{\Psi}_f \gamma^\mu \gamma_5 \Psi_f \partial_\mu \phi_A\,. \qquad (7)$$

Here, Ψ_f is the fermion field, m_f its mass, and C_f a model-dependent coefficient. The dimensionless combination $g_{Aff} \equiv C_f m_f / f_A$ plays the role of a Yukawa coupling and $\alpha_{Aff} \equiv g_{Aff}^2 / 4\pi$ of a "fine-structure constant." The often-used pseudoscalar form $\mathcal{L}_{Aff} = -\mathrm{i}\,(C_f m_f / f_A)\,\bar{\Psi}_f \gamma_5 \Psi_f \phi_A$ need not be equivalent to the appropriate derivative structure, for example when two NG bosons are attached to one fermion line as in axion emission by nucleon bremsstrahlung [17].

In the DFSZ model [15], the tree-level coupling coefficient to electrons is

$$C_e = \frac{\cos^2 \beta}{3}\,, \qquad (8)$$

where $\tan\beta$ is the ratio of two Higgs vacuum expectation values that are generic to this and similar models.

For nucleons, $C_{n,p}$ are related to axial-vector current matrix elements by generalized Goldberger-Treiman relations,

$$\begin{aligned}
C_p &= (C_u - \eta)\Delta u + (C_d - \eta z)\Delta d + (C_s - \eta w)\Delta s\,,\\
C_n &= (C_u - \eta)\Delta d + (C_d - \eta z)\Delta u + (C_s - \eta w)\Delta s\,.
\end{aligned} \qquad (9)$$

Here, $\eta = (1 + z + w)^{-1}$ with $z = m_u/m_d$ and $w = m_u/m_s \ll z$ and the Δq are given by the axial vector current matrix element $\Delta q\, S_\mu = \langle p|\bar{q}\gamma_\mu\gamma_5 q|p\rangle$ with S_μ the proton spin.

Neutron beta decay and strong isospin symmetry considerations imply $\Delta u - \Delta d = F + D = 1.269 \pm 0.003$, whereas hyperon

decays and flavor SU(3) symmetry imply $\Delta u + \Delta d - 2\Delta s = 3F - D = 0.586 \pm 0.031$ [19]. The strange-quark contribution is $\Delta s = -0.08 \pm 0.01_{\text{stat}} \pm 0.05_{\text{syst}}$ from the COMPASS experiment [18], and $\Delta s = -0.085 \pm 0.008_{\text{exp}} \pm 0.013_{\text{theor}} \pm 0.009_{\text{evol}}$ from HERMES [19], in agreement with each other and with an early estimate of $\Delta s = -0.11 \pm 0.03$ [20]. We thus adopt $\Delta u = 0.84 \pm 0.02$, $\Delta d = -0.43 \pm 0.02$ and $\Delta s = -0.09 \pm 0.02$, very similar to what was used in the axion literature.

The uncertainty of the axion-nucleon couplings is dominated by the uncertainty $z = m_u/m_d = 0.35\text{–}0.60$ that we mentioned earlier. For hadronic axions $C_{u,d,s} = 0$ so that $-0.51 < C_p < -0.36$ and $0.10 > C_n > -0.05$. Therefore it is well possible that $C_n = 0$ whereas C_p does not vanish within the plausible z range. In the DFSZ model, $C_u = \frac{1}{3}\sin^2\beta$ and $C_d = \frac{1}{3}\cos^2\beta$ and C_n and C_p as functions of β and z do not vanish simultaneously.

The axion-pion interaction is given by the Lagrangian [21]

$$\mathcal{L}_{A\pi} = \frac{C_{A\pi}}{f_\pi f_A} \left(\pi^0\pi^+\partial_\mu\pi^- + \pi^0\pi^-\partial_\mu\pi^+ - 2\pi^+\pi^-\partial_\mu\pi^0\right)\partial_\mu\phi_A,$$
(10)

where $C_{A\pi} = (1-z)/[3(1+z)]$ in hadronic models. The chiral symmetry-breaking Lagrangian provides an additional term $\mathcal{L}'_{A\pi} \propto (m_\pi^2/f_\pi f_A)(\pi^0\pi^0 + 2\pi^-\pi^+)\pi^0\phi_A$. For hadronic axions it vanishes identically, in contrast to the DFSZ model (Roberto Peccei, private communication).

II. LABORATORY SEARCHES

II.1 Photon regeneration

Searching for "invisible axions" is extremely challenging. The most promising approaches rely on the axion-two-photon vertex, allowing for axion-photon conversion in external electric or magnetic fields [5]. For the Coulomb field of a charged particle, the conversion is best viewed as a scattering process, $\gamma + Ze \leftrightarrow Ze + A$, called Primakoff effect [22]. In the other extreme of a macroscopic field, usually a large-scale B-field, the momentum transfer is small, the interaction coherent over a large distance, and the conversion is best viewed as an axion-photon oscillation phenomenon in analogy to neutrino flavor oscillations [23].

Photons propagating through a transverse magnetic field, with incident $\mathbf{E}_\gamma$ and magnet $\mathbf{B}$ parallel, may convert into axions. For $m_A^2 L/2\omega \ll 2\pi$, where L is the length of the B field region and ω the photon energy, the resultant axion beam is coherent with the incident photon beam and the conversion probability is $\Pi \sim (1/4)(G_{A\gamma\gamma}BL)^2$. A practical realization uses a laser beam propagating down the bore of a superconducting dipole magnet (like the bending magnets in high-energy accelerators). If another magnet is in line with the first, but shielded by an optical barrier, then photons may be regenerated from the pure axion beam [24]. The overall probability $P(\gamma \to A \to \gamma) = \Pi^2$.

The first such experiment utilized two magnets of length $L = 4.4$ m and $B = 3.7$ T and found $G_{A\gamma\gamma} < 6.7 \times 10^{-7}$ GeV^{-1} at 95% CL for $m_A < 1$ meV [25]. More recently, several such experiments were performed (see Listings), improving the limit to $G_{A\gamma\gamma} < 3.5 \times 10^{-7}$ GeV^{-1} at 3σ in the massless limit [26]. Some of these experiments have also reported limits for scalar bosons where the photon $\mathbf{E}_\gamma$ must be chosen perpendicular to the magnet $\mathbf{B}$.

A new concept, resonantly-enhanced photon regeneration, may open unexplored regions of coupling strength [27]. In this scheme, both the production and detection magnets are within Fabry-Perot optical cavities and actively locked in frequency. The $\gamma \to A \to \gamma$ rate is enhanced by a factor $2\mathcal{F}\mathcal{F}'/\pi^2$ relative to a single-pass experiment, where $\mathcal{F}$ and $\mathcal{F}'$ are the finesses of the two cavities. The resonant enhancement could be of order $10^{(10-12)}$, improving the $G_{A\gamma\gamma}$ sensitivity by $10^{(2.5-3)}$. Another new concept involves axion absorption and emission between electromagnetic fields within a high finesse optical cavity [28]. A signal appears as resonant sidebands on the carrier. This technique could be sensitive in the mass range 10^{-6}–10^{-4} eV and reach the KSVZ line after one year of operation.

II.2 Photon polarization

An alternative to regenerating the lost photons is to use the beam itself to detect conversion: the polarization of light propagating through a transverse B field suffers dichroism and birefrigence [29]. Dichroism: The $E_\parallel$ component, but not $E_\perp$,

is depleted by axion production, causing a small rotation of linearly polarized light. For $m_A^2 L/2\omega \ll 2\pi$ the effect is independent of m_A, for heavier axions it oscillates and diminishes as m_A increases, and it vanishes for $m_A > \omega$. Birefringence: This rotation occurs because there is mixing of virtual axions in the $E_\parallel$ state, but not for $E_\perp$. Hence, linearly polarized light will develop elliptical polarization. Higher-order QED also induces vacuum birefringence. A search for these effects was performed on the same dipole magnets in the early experiment above [30]. The dichroic rotation gave a stronger limit than the ellipticity rotation: $G_{A\gamma\gamma} < 3.6 \times 10^{-7}$ GeV^{-1} at 95% CL for $m_A < 5 \times 10^{-4}$ eV. The ellipticity limits are better at higher masses, as they fall off smoothly and do not terminate at m_A.

In 2006 the PVLAS collaboration reported a signature of magnetically induced vacuum dichroism that could be interpreted as the effect of a pseudoscalar with $m_A = 1\text{–}1.5$ meV and $G_{A\gamma\gamma} = (1.6\text{–}5) \times 10^{-6}$ GeV^{-1} [31]. Since then, these findings are attributed to instrumental artifacts [32]. This particle interpretation is also excluded by the above photon regeneration searches that were triggered by the original PVLAS result.

II.3 Long-range forces

New bosons would mediate long-range forces, which are severely constrained by "fifth force" experiments [33]. Those looking for new mass-spin couplings provide significant constraints on pseudoscalar bosons [34]. However, they do not yet cover realistic parameters for invisible axion models because they are only sensitive for small m_A. The corresponding coupling strengths scale with $f_A^{-1} \approx m_A/m_\pi f_\pi$ and are too small to be detected. Still, these efforts provide constraints on more general low-mass bosons.

III. AXIONS FROM ASTROPHYSICAL SOURCES

III.1 Stellar energy-loss limits:

Low-mass weakly-interacting particles (neutrinos, gravitons, axions, baryonic or leptonic gauge bosons, *etc.*) are produced in hot astrophysical plasmas, and can thus transport energy out of stars. The coupling strength of these particles with normal matter and radiation is bounded by the constraint

that stellar lifetimes or energy-loss rates not conflict with observation [35–37].

We begin this discussion with our Sun and concentrate on hadronic axions. They are produced predominantly by the Primakoff process $\gamma + Ze \to Ze + A$. Integrating over a standard solar model yields the axion luminosity [49]

$$L_A = G_{10}^2 \, 1.85 \times 10^{-3} \, L_\odot \, , \tag{11}$$

where $G_{10} = G_{A\gamma\gamma} \times 10^{10}$ GeV. The maximum of the spectrum is at 3.0 keV, the average at 4.2 keV, and the number flux at Earth is $G_{10}^2 \, 3.75 \times 10^{11}$ cm^{-2} s^{-1}. The solar photon luminosity is fixed, so axion losses require enhanced nuclear energy production and thus enhanced neutrino fluxes. The all-flavor measurements by SNO together with a standard solar model imply $L_A \lesssim 0.10 \, L_\odot$, corresponding to $G_{10} \lesssim 7$ [38], mildly superseding a similar limit from helioseismology [39].

A more restrictive limit derives from globular-cluster (GC) stars that allow for detailed tests of stellar-evolution theory. The stars on the horizontal branch (HB) in the color-magnitude diagram have reached helium burning with a core-averaged energy release of about 80 erg g^{-1} s^{-1}, compared to Primakoff axion losses of $G_{10}^2 \, 30$ erg g^{-1} s^{-1}. The accelerated consumption of helium reduces the HB lifetime by about $80/(80 + 30 \, G_{10}^2)$. Number counts of HB stars in 15 GCs compared with the number of red giants (that are not much affected by Primakoff losses) reveal agreement with expectations within 20–40% in any one GC and overall on the 10% level [36]. Therefore, a reasonably conservative limit is

$$G_{A\gamma\gamma} \lesssim 1 \times 10^{-10} \text{ GeV}^{-1} \, , \tag{12}$$

although a detailed error budget is not available.

We translate this constraint on $G_{A\gamma\gamma}$ to $f_A > 2.3 \times 10^7$ GeV ($m_A < 0.3$ eV), using $z = 0.56$ and $E/N = 0$ as in the KSVZ model, and show the excluded range in Figure 1. For the DFSZ model with $E/N = 8/3$, the corresponding limits are slightly less restrictive, $f_A > 0.8 \times 10^7$ GeV ($m_A < 0.7$ eV). The exact high-mass end of the exclusion range has not been determined. The relevant temperature is around 10 keV and the average

photon energy is therefore around 30 keV. The excluded m_A range thus certainly extends beyond the shown 100 keV.

If axions couple directly to electrons, the dominant emission processes are $\gamma + e^- \rightarrow e^- + A$ and $e^- + Ze \rightarrow Ze + e^- + A$. Moreover, bremsstrahlung is efficient in white dwarfs (WDs), where the Primakoff and Compton processes are suppressed by the large plasma frequency. The enhanced energy losses would delay helium ignition in GC stars, implying $\alpha_{Aee} \lesssim 0.5 \times 10^{-26}$ [40]. Enhanced WD cooling leads to a similar limit from the WD luminosity function [41]. For pulsationally unstable WDs (ZZ Ceti stars), the period decrease $\dot{P}/P$ is a measure of the cooling speed. A well-studied case is the star G117–B15A, where the measured $\dot{P}/P$ implies [42]

$$\alpha_{Aee} < 1.3 \times 10^{-27} \tag{13}$$

at a statistical 95% CL. (We have corrected the published limit for an apparent misprint.) This result is equivalent to $g_{Aee} < 1.3 \times 10^{-13}$ or in the DFSZ model to $f_A > 1.3 \times 10^9$ GeV $\cos^2\beta$ and $m_A < 4.5$ meV/$\cos^2\beta$. We show these constraints in Figure 1 for $\cos^2\beta = 1/2$.

Similar constraints derive from the measured duration of the neutrino signal of the supernova SN 1987A. Numerical simulations for a variety of cases, including axions and Kaluza-Klein gravitons, reveal that the energy-loss rate of a nuclear medium at the density 3×10^{14} g cm^{-3} and temperature 30 MeV should not exceed about 1×10^{19} erg g^{-1} s^{-1} [36]. The energy-loss rate from nucleon bremsstrahlung, $N + N \rightarrow N + N + A$, is $(C_N/2f_A)^2 (T^4/\pi^2 m_N) F$. Here F is a numerical factor that represents an integral over the dynamical spin-density structure function because axions couple to the nucleon spin. For realistic conditions, even after considerable effort, one is limited to a heuristic estimate leading to $F \approx 1$ [37].

The SN 1987A limits are of particular interest for hadronic axions where the bounds on α_{Aee} are moot. Within uncertainties of $z = m_u/m_d$ a reasonable choice for the coupling constants is then $C_p = -0.4$ and $C_n = 0$. Using a proton fraction of 0.3, $F = 1$, and $T = 30$ MeV one finds [37]

$$f_A \gtrsim 4 \times 10^8 \text{ GeV} \qquad \text{and} \qquad m_A \lesssim 16 \text{ meV} . \tag{14}$$
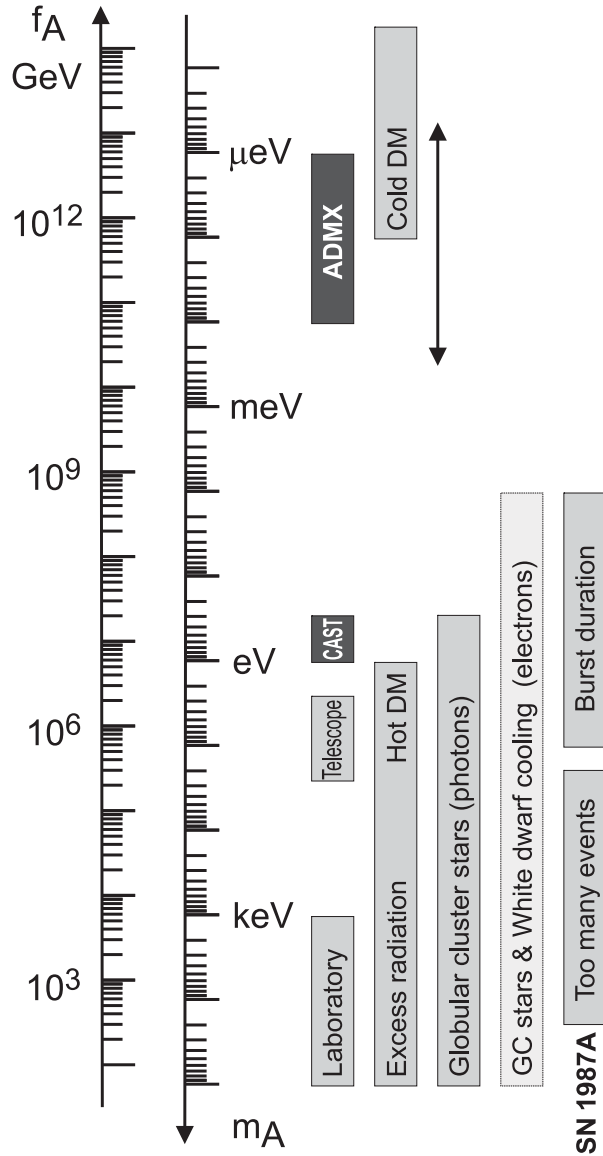
Figure 1: Exclusion ranges as described in the text. The dark intervals are the approximate CAST and ADMX search ranges. Limits on coupling strengths are translated into limits on m_A and f_A using $z = 0.56$ and the KSVZ values for the coupling strengths. The "Laboratory" bar is a rough representation of the exclusion range for standard or variant axions. The "GC stars and white-dwarf cooling" range uses the DFSZ model with an axion-electron coupling corresponding to $\cos^2 \beta = 1/2$. The Cold Dark Matter exclusion range is particularly uncertain. We show the benchmark case from the misalignment mechanism.

If axions interact sufficiently strongly they are trapped. Only about three orders of magnitude in g_{ANN} or m_A are excluded, a range shown somewhat schematically in Figure 1. For even larger couplings, the axion flux would have been negligible, yet it would have triggered additional events in the detectors, excluding a further range [43]. A possible gap between these two SN 1987A arguments was discussed as the "hadronic axion window" under the assumption that $G_{A\gamma\gamma}$ was anomalously small [44]. This range is now excluded by hot dark matter bounds (see below).

III.2 Searches for solar axions

Instead of using stellar energy losses to derive axion limits, one can also search directly for these fluxes, notably from the Sun. The main focus has been on axion-like particles with a two-photon vertex. They are produced by the Primakoff process with a flux given by Equation 11 and can be detected at Earth with the reverse process in a macroscopic B-field ("axion helioscope") [5]. The average energy of solar axions of 4.2 keV implies a photon-axion oscillation length in vacuum of $2\pi \left(2\omega/m_A^2\right) \sim \mathcal{O}(1 \text{ mm})$, precluding the vacuum mixing from achieving its theoretical maximum in any practical magnet. However, one can endow the photon with an effective mass in a gas, $m_\gamma = \omega_{\text{plas}}$, thus matching the axion and photon dispersion relations [45].

An early implementation of these ideas used a conventional dipole magnet, with a conversion volume of variable-pressure gas with a xenon proportional chamber as x-ray detector [46]. The conversion magnet was fixed in orientation and collected data for about 1000 s/day. Axions were excluded for $G_{A\gamma\gamma} < 3.6 \times 10^{-9}$ GeV^{-1} for $m_A < 0.03$ eV, and $G_{A\gamma\gamma} < 7.7 \times 10^{-9}$ GeV^{-1} for $0.03 < m_A < 0.11$ eV at 95% CL.

Later, the Tokyo axion helioscope used a superconducting magnet on a tracking mount, viewing the Sun continuously. They reported $G_{A\gamma\gamma} < 6 \times 10^{-10}$ GeV^{-1} for $m_A < 0.3$ eV [47]. Recently this experiment was recommissioned and a similar limit for masses around 1 eV was reported [48]. These exclusion ranges are shown in Figure 2.
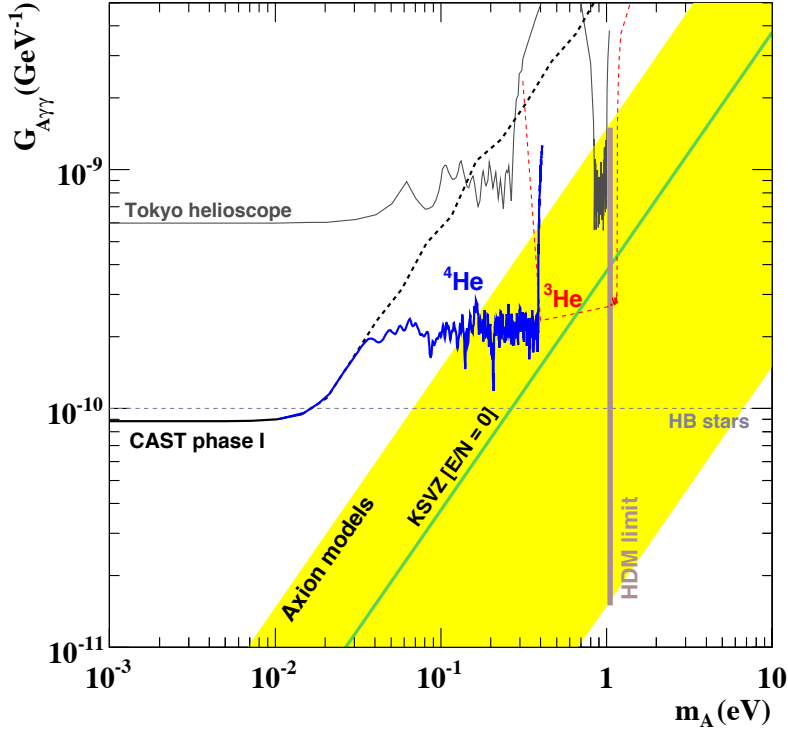
Figure 2: Solar exclusion plot for axion-like particles [50]. The red dashed line is the sensitivity of the ongoing ^{3}He phase of CAST. The vertical line (HDM) is the hot dark-matter limit [59]. The yellow band represents models with $0.07 < |E/N - 1.92| < 0.7$, the green solid line corresponds to KSVZ axions.

The most recent helioscope CAST (CERN Axion Solar Telescope) uses a decommissioned LHC dipole magnet on a tracking mount. The hardware includes grazing-incidence x-ray optics with solid-state x-ray detectors, as well as a novel x-ray Micromegas position-sensitive gaseous detector. CAST has established a 95% CL limit $G_{A\gamma\gamma} < 8.8 \times 10^{-11}$ GeV^{-1} for $m_A < 0.02$ eV [49]. To cover larger masses and to "cross the axion line," the magnet bores are filled with a gas at varying pressure. The runs with ^{4}He cover masses up to about 0.4 eV [50], providing the limits shown in Figure 2. Ongoing runs with ^{3}He gas have explored masses up to 0.85 eV, aiming to about 1.16 eV, but final results are not yet available.

Other Primakoff searches for solar axions have been carried out using crystal detectors, exploiting the coherent conversion of axions into photons when the axion angle of incidence satisfies a Bragg condition with a crystal plane [51]. However, none of these limits is more restrictive than the one derived from solar neutrinos that was discussed earlier.

Another idea is to look at the Sun with an x-ray satellite when the Earth is in between. Solar axions would convert in the Earth magnetic field on the far side and could be detected [52]. The sensitivity to $G_{A\gamma\gamma}$ could be comparable to CAST, but only for much smaller m_A.

III.3 Conversion of astrophysical photon fluxes

Large-scale B fields exist in astrophysics that can induce axion-photon oscillations. In practical cases, B is much smaller than in the laboratory, whereas the conversion region L is much larger. Therefore, while the product BL can be large, realistic sensitivities are usually restricted to very low-mass particles, far away from the "axion line" in a plot like Figure 2.

One example is SN 1987A, which would have emitted a burst of axion-like particles due to the Primakoff production in its core. They would have partially converted into γ-rays in the galactic B-field. The absence of a γ-ray burst in coincidence with SN 1987A neutrinos provides a limit $G_{A\gamma\gamma} \lesssim 1 \times 10^{-11}$ GeV^{-1} for $m_A \lesssim 10^{-9}$ eV [53], the most restrictive limit for very small m_A. Axion-like particles from other stars can be converted to photons, but no tangible new limits or signatures seem to have appeared.

Conversely, photons from distant sources could transform to axion-like particles, depleting the original flux. This mechanism was proposed as an alternative to cosmic acceleration for explaining the apparent dimming of distant SNe Ia [54]. However, this effect would apply to all distant sources, including quasars and the cosmic microwave background and would depend on energy. All things considered, this mechanism can only play a subdominant role [55]. On the other hand, very recently the observed scatter of x/γ-ray fluxes from active galactic nuclei was interpreted in terms of very low-mass ALPs [56].

High-energy γ-rays are typically produced in magnetized environments where cosmic rays are accelerated. The conversion into axion-like particles can then, in principle, imprint observable features on the spectrum for a range of coupling constants not excluded by other arguments [57].

IV. COSMIC AXIONS

IV.1 Cosmic axion populations

In the early universe, axions are produced by processes involving quarks and gluons [58]. After color confinement, the dominant thermalization process is $\pi + \pi \leftrightarrow \pi + A$ [21]. The resulting axion population would contribute a hot dark matter component in analogy to massive neutrinos. Cosmological precision data provide restrictive constraints on a possible hot dark-matter fraction that translate into $m_A < 0.4$–1.0 eV at the 95% statistical CL [59]. The spread of published limits reflects the use of different cosmological data sets.

For $m_A \gtrsim 20$ eV, axions decay fast on a cosmic time scale, removing the axion population while injecting photons. This excess radiation provides additional limits up to very large axion masses [60]. An anomalously small $G_{A\gamma\gamma}$ provides no loophole because suppressing decays leads to thermal axions overdominating the mass density of the universe.

The main cosmological interest in axions derives from their possible role as cold dark matter (CDM). In addition to thermal processes, axions are abundantly produced by the "misalignment mechanism" [61]. After the breakdown of the PQ symmetry, the axion field relaxes somewhere in the "bottom of the wine bottle" potential. Near the QCD epoch, instanton effects explicitly break the PQ symmetry, the very effect that causes dynamical PQ symmetry restoration. This "tilting of the wine bottle" drives the axion field toward the CP-conserving minimum, thereby exciting coherent oscillations of the axion field that ultimately represent a condensate of CDM. The cosmic mass density in this homogeneous field mode is [62]

$$\Omega_A h^2 \approx 0.7 \left(\frac{f_A}{10^{12}\ \text{GeV}} \right)^{7/6} \left(\frac{\bar{\Theta}_{\text{i}}}{\pi} \right)^2 , \qquad (15)$$

where h is the present-day Hubble expansion parameter in units of 100 km s^{-1} Mpc^{-1}, and $-\pi \leq \bar{\Theta}_i \leq \pi$ is the initial "misalignment angle" relative to the CP-conserving position. If the PQ symmetry breakdown takes place after inflation, $\bar{\Theta}_i$ will take on different values in different patches of the universe. The average contribution is [62]

$$\Omega_A h^2 \approx 0.3 \left(\frac{f_A}{10^{12} \text{ GeV}} \right)^{7/6} . \tag{16}$$

Comparing with the measured CDM density of $\Omega_{\text{CDM}} h^2 \approx 0.13$ implies that axions with $m_A \approx 10 \ \mu$eV provide the dark matter, whereas smaller masses are excluded (Figure 1).

This density sets only a rough scale for the expected m_A. The mass of CDM axions could be significantly smaller or larger than 10 μeV. Apart from the overall particle physics uncertainties, the cosmological sequence of events is crucial. Assuming axions make up CDM, much smaller masses are possible if inflation took place after the PQ transition and the initial value $\bar{\Theta}_i$ was small ("anthropic axion window" [63]). Conversely, if the PQ transition took place after inflation, there are additional sources for nonthermal axions, notably the decay of cosmic strings and domain walls, although these populations are comparable to the misalignment contribution [62].

If the reheat temperature after inflation is too small to restore PQ symmetry, the axion field is present during inflation. It is subject to quantum fluctuations, leading to isocurvature fluctuations that are severely constrained [64].

In the opposite case without inflation after the PQ transition, the spatial axion density variations are large at the QCD transition and they are not erased by free streaming. When matter begins to dominate the universe, gravitationally bound "axion mini clusters" form promptly [65]. A significant fraction of CDM axions can reside in these bound objects.

IV.2 Telescope searches

The two-photon decay is extremely slow for axions with masses in the CDM regime, but could be detectable for eV masses. The signature would be a quasi-monochromatic emission line from galaxies and galaxy clusters. The expected optical line intensity for DFSZ axions is similar to the continuum night emission. An early search in three rich Abell clusters [66], and a recent search in two rich Abell clusters [67], exclude the "Telescope" range in Figure 1 unless the axion-photon coupling is strongly suppressed. Of course, axions in this mass range would anyway provide an excessive hot DM contribution.

Very low-mass axions in halos produce a weak quasi-monochromatic radio line. Virial velocities in undisrupted dwarf galaxies are very low, and the axion decay line would therefore be extremely narrow. A search with the Haystack radio telescope on three nearby dwarf galaxies provided a limit $G_{A\gamma\gamma} < 1.0 \times 10^{-9}$ GeV^{-1} at 96% CL for $298 < m_A < 363$ μeV [68]. However, this combination of m_A and $G_{A\gamma\gamma}$ does not exclude plausible axion models.

IV.3 Microwave cavity experiments

The limits of Figure 1 suggest that axions, if they exist, provide a significant fraction or even perhaps all of the cosmic CDM. In a broad range of the plausible m_A range for CDM, galactic halo axions may be detected by their resonant conversion into a quasi-monochromatic microwave signal in a high-Q electromagnetic cavity permeated by a strong static B field [5,69]. The cavity frequency is tunable, and the signal is maximized when the frequency is the total axion energy, rest mass plus kinetic energy, of $\nu = (m_A/2\pi)\,[1 + \mathcal{O}(10^{-6})]$, the width above the rest mass representing the virial distribution in the galaxy. The frequency spectrum may also contain finer structure from axions more recently fallen into the galactic potential and not yet completely virialized [70].
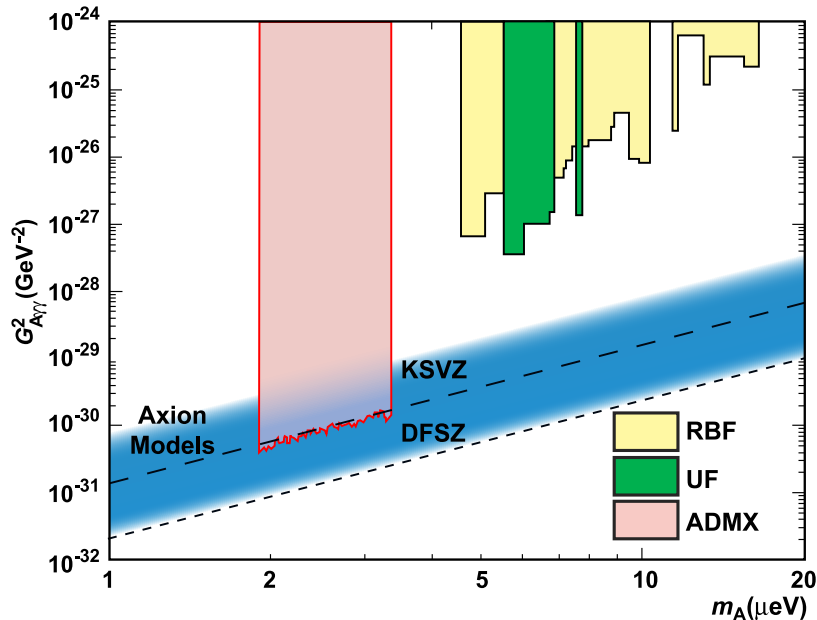
Figure 3: Exclusion region reported from the microwave cavity experiments RBF and UF [71] and ADMX [72]. A local dark-matter density of 450 MeV cm^{-3} is assumed.

The feasibility of this technique was established in early experiments of relatively small sensitive volume, $\mathcal{O}(1$ liter), with HFET-based amplifiers, setting limits in the range $4.5 < m_A < 16.3$ μeV [71], but lacking by 2–3 orders of magnitude the sensitivity required to detect realistic axions. Later, ADMX ($B \sim 8$ T, $V \sim 200$ liters) has achieved sensitivity to KSVZ axions, assuming they saturate the local dark matter density and are well virialized, over the mass range 1.9–3.3 μeV [72]. Should halo axions have a component not yet virialized, ADMX is sensitive to DFSZ axions [73]. The corresponding 90% CL exclusion regions shown in Figure 3 are normalized to an assumed local CDM density of 7.5×10^{-25} g cm^{-3} (450 MeV cm^{-3}). Very recently the ADMX experiment has commissioned an upgrade [74] that replaces the microwave HFET amplifiers by near quantum-limited low-noise dc SQUID microwave amplifiers [75], allowing for a significantly improved sensitivity. Alternatively, a Rydberg atom single-photon detector [76] can in principle evade

the standard quantum limit for coherent photon detection. Efforts are underway to incorporate Rydberg atom systems in RF cavity axion searches [77].

Conclusions

Experimental, astrophysical, and cosmological limits have been refined and indicate that axions, if they exist, very likely have very low mass, $m_A \lesssim 10$ meV, suggesting that axions are a non-negligible fraction of the cosmic CDM. The upgraded versions of the ADMX experiment will ultimately cover the range 1–100 μeV with a sensitivity allowing one to detect such axions, unless the local DM density is unexpectedly small or the axion-photon coupling anomalously weak. Other experimental techniques remain of interest to search for axion-like particles, although at present no method besides the DM search is known that could detect realistic axions obeying the astrophysical and cosmological limits, and fulfilling the QCD-implied relationship between mass and coupling strength.

References

1. R.D. Peccei and H. Quinn, Phys. Rev. Lett. **38**, 1440 (1977), Phys. Rev. **D16**, 1791 (1977).

2. S. Weinberg, Phys. Rev. Lett. **40**, 223 (1978);
   F. Wilczek, Phys. Rev. Lett. **40**, 279 (1978).

3. F. Wilczek, Phys. Rev. Lett. **49**, 1549 (1982).

4. Y. Chikashige, R.N. Mohapatra, and R.D. Peccei, Phys. Lett. **98B**, 265 (1981);
   G.B. Gelmini and M. Roncadelli, Phys. Lett. **99B**, 411 (1981).

5. P. Sikivie, Phys. Rev. Lett. **51**, 1415 (1983) and Erratum *ibid.*, **52**, 695 (1984).

6. C.A. Baker *et al.*, Phys. Rev. Lett. **97**, 131801 (2006).

7. H. Georgi, D.B. Kaplan, and L. Randall, Phys. Lett. **B169**, 73 (1986).

8. H. Leutwyler, Phys. Lett. **B378**, 313 (1996).

9. Mini review on Quark Masses in: C. Amsler *et al.* (Particle Data Group), Phys. Lett. **B667**, 1 (2008).

10. T.W. Donnelly *et al.*, Phys. Rev. **D18**, 1607 (1978);
    S. Barshay *et al.*, Phys. Rev. Lett. **46**, 1361 (1981);
    A. Barroso and N.C. Mukhopadhyay, Phys. Lett. **B106**, 91 (1981);

R.D. Peccei, in *Proceedings of Neutrino '81*, Honolulu, Hawaii, Vol. 1, p. 149 (1981);
L.M. Krauss and F. Wilczek, Phys. Lett. **B173**, 189 (1986).

11.   J. Schweppe *et al.*, Phys. Rev. Lett. **51**, 2261 (1983);
T. Cowan *et al.*, Phys. Rev. Lett. **54**, 1761 (1985).

12.   R.D. Peccei, T.T. Wu, and T. Yanagida, Phys. Lett. **B172**, 435 (1986).

13.   W.A. Bardeen, R.D. Peccei, and T. Yanagida, Nucl. Phys. **B279**, 401 (1987).

14.   J.E. Kim, Phys. Rev. Lett. **43**, 103 (1979);
M.A. Shifman, A.I. Vainstein, and V.I. Zakharov, Nucl. Phys. **B166**, 493 (1980).

15.   M. Dine, W. Fischler, and M. Srednicki, Phys. Lett. **B104**, 199 (1981);
A.R. Zhitnitsky, Sov. J. Nucl. Phys. **31**, 260 (1980).

16.   S.L. Cheng, C.Q. Geng, and W.T. Ni, Phys. Rev. **D52**, 3132 (1995).

17.   G. Raffelt and D. Seckel, Phys. Rev. Lett. **60**, 1793 (1988);
M. Carena and R.D. Peccei, Phys. Rev. **D40**, 652 (1989);
K. Choi, K. Kang, and J.E. Kim, Phys. Rev. Lett. **62**, 849 (1989).

18.   V.Y. Alexakhin *et al.* (COMPASS Collab.), Phys. Lett. **B647**, 8 (2007).

19.   A. Airapetian *et al.* (HERMES Collab.), Phys. Rev. **D75**, 012007 (2007) and Erratum *ibid.*, **D76**, 039901 (2007).

20.   J.R. Ellis and M. Karliner, in: *The spin structure of the nucleon: International school of nucleon structure* (3–10 August 1995, Erice, Italy), ed. by B. Frois, V.W. Hughes, and N. De Groot (World Scientific, Singapore, 1997) [hep-ph/9601280].

21.   S. Chang and K. Choi, Phys. Lett. **B316**, 51 (1993).

22.   D.A. Dicus *et al.*, Phys. Rev. **D18**, 1829 (1978).

23.   G. Raffelt and L. Stodolsky, Phys. Rev. **D37**, 1237 (1988).

24.   K. van Bibber *et al.*, Phys. Rev. Lett. **59**, 759 (1987).

25.   G. Ruoso *et al.*, Z. Phys. **C56**, 505 (1992);
R. Cameron *et al.*, Phys. Rev. **D47**, 3707 (1993).

26.   M. Fouche *et al.*, Phys. Rev. **D78**, 032013 (2008);
A.S. Chou *et al.* (GammeV Collab.), Phys. Rev. Lett. **100**, 080402 (2008);
A. Afanasev *et al.*, Phys. Rev. Lett. **101**, 120401 (2008);
K. Ehret *et al.* (ALPS Collab.), Nucl. Instrum. Methods **A612**, 83 (2009).

27. P. Sikivie, D. Tanner, and K. van Bibber, Phys. Rev. Lett. **98**, 172002 (2007);
     G. Mueller *et al.*, Phys. Rev. **D80**, 072004 (2009).

28. A. Melissinos, Phys. Rev. Lett. **102**, 202001 (2009).

29. L. Maiani *et al.*, Phys. Lett. **B175**, 359 (1986).

30. Y. Semertzidis *et al.*, Phys. Rev. Lett. **64**, 2988 (1990).

31. E. Zavattini *et al.* (PVLAS Collab.), Phys. Rev. Lett. **96**, 110406 (2006).

32. E. Zavattini *et al.* (PVLAS Collab.), Phys. Rev. **D77**, 032006 (2008).

33. E. Fischbach and C. Talmadge, Nature **356**, 207 (1992).

34. J.E. Moody and F. Wilczek, Phys. Rev. D 30, 130(1984);
     A.N. Youdin *et al.*, Phys. Rev. Lett. **77**, 2170 (1996);
     Wei-Tou Ni *et al.*, Phys. Rev. Lett. **82**, 2439 (1999);
     D.F. Phillips *et al.*, Phys. Rev. **D63**, 111101 (R)(2001);
     B.R. Heckel *et al.* (Eöt-Wash Collab.), Phys. Rev. Lett. **97**, 021603 (2006).

35. M.S. Turner, Phys. Reports **197**, 67 (1990);
     G.G. Raffelt, Phys. Reports **198**, 1 (1990).

36. G.G. Raffelt, *Stars as Laboratories for Fundamental Physics*, (Univ. of Chicago Press, Chicago, 1996).

37. G.G. Raffelt, Lect. Notes Phys. **741**, 51 (2008).

38. P. Gondolo and G. Raffelt, Phys. Rev. **D79**, 107301 (2009).

39. H. Schlattl, A. Weiss, and G. Raffelt, Astropart. Phys. **10**, 353 (1999).

40. G. Raffelt and A. Weiss, Phys. Rev. **D51**, 1495 (1995);
     M. Catelan, J.A. de Freitas Pacheco, and J.E. Horvath, Astrophys. J. **461**, 231 (1996).

41. G.G. Raffelt, Phys. Lett. **B166**, 402 (1986);
     S.I. Blinnikov and N.V. Dunina-Barkovskaya, Mon. Not. R. Astron. Soc. **266**, 289 (1994);
     J. Isern *et al.*, J. Phys. Conf. Ser. **172**, 012005 (2009).

42. A.H. Córsico *et al.*, New Astron. **6**, 197 (2001);
     J. Isern and E. García-Berro, Nucl. Phys. B Proc. Suppl. **114**, 107 (2003).

43. J. Engel, D. Seckel, and A.C. Hayes, Phys. Rev. Lett. **65**, 960 (1990).

44. T. Moroi and H. Murayama, Phys. Lett. **B440**, 69 (1998).

45. K. van Bibber *et al.*, Phys. Rev. **D39**, 2089 (1989).

46. D. Lazarus *et al.*, Phys. Rev. Lett. **69**, 2333 (1992).

47. S. Moriyama *et al.*, Phys. Lett. **B434**, 147 (1998);
     Y. Inoue *et al.*, Phys. Lett. **B536**, 18 (2002).

48. M. Minowa *et al.*, Phys. Lett. **B668**, 93 (2008).

49. S. Andriamonje *et al.* (CAST Collab.), JCAP **0704**, 010 (2007).

50. E. Arik *et al.* (CAST Collab.), JCAP **0902**, 008 (2009).

51. F.T. Avignone III *et al.*, Phys. Rev. Lett. **81**, 5068 (1998);
     A. Morales *et al.* (COSME Collab.), Astropart. Phys. **16**, 325 (2002);
     R. Bernabei *et al.*, Phys. Lett. **B515**, 6 (2001);
     Z. Ahmed *et al.* (CDMS Collab.), Phys. Rev. Lett. **103**, 141802 (2009).

52. H. Davoudiasl and P. Huber, Phys. Rev. Lett. **97**, 141302 (2006).

53. J.W. Brockway, E.D. Carlson, and G.G. Raffelt, Phys. Lett. **B383**, 439 (1996);
     J.A. Grifols, E.Massó, and R. Toldrà, Phys. Rev. Lett. **77**, 2372 (1996).

54. C. Csaki, N. Kaloper, and J. Terning, Phys. Rev. Lett. **88**, 161302 (2002).

55. A. Mirizzi, G.G. Raffelt, and P.D. Serpico, Lect. Notes Phys. **741**, 115 (2008).

56. C. Burrage, A.C. Davis and D.J. Shaw, Phys. Rev. Lett. **102**, 201101 (2009).

57. D. Hooper and P.D. Serpico, Phys. Rev. Lett. **99**, 231102 (2007);
     K.A. Hochmuth and G. Sigl, Phys. Rev. **D76**, 123011 (2007);
     A. De Angelis, O. Mansutti and M. Roncadelli, Phys. Rev. **D76**, 121301 (2007);
     A. Mirizzi and D. Montanino, JCAP **0912**, 004 (2009).

58. M.S. Turner, Phys. Rev. Lett. **59**, 2489 (1987) and Erratum *ibid.*, **60**, 1101 (1988);
     E. Massó, F. Rota, and G. Zsembinszki, Phys. Rev. **D66**, 023004 (2002).

59. A. Melchiorri, O. Mena, and A. Slosar, Phys. Rev. **D76**, 041303 (2007);
     S. Hannestad *et al.*, JCAP **0804**, 019 (2008).

60. E. Massó and R. Toldra, Phys. Rev. **D55**, 7967 (1997).

61. J. Preskill, M.B. Wise, and F. Wilczek, Phys. Lett. **B120**, 127 (1983);
     L.F. Abbott and P. Sikivie, Phys. Lett. **B120**, 133 (1983);
     M. Dine and W. Fischler, Phys. Lett. **B120**, 137 (1983).

62. P. Sikivie, Lect. Notes Phys. **741**, 19 (2008).

63. M. Tegmark *et al.*, Phys. Rev. **D73**, 023505 (2006).

64. M. Beltrán, J. García-Bellido, and J. Lesgourgues, Phys. Rev. **D75**, 103507 (2007);
M.P. Hertzberg, M. Tegmark and F. Wilczek, Phys. Rev. **D78**, 083507 (2008);
J. Hamann *et al.*, JCAP **0906**, 022 (2009).

65. E.W. Kolb and I.I. Tkachev, Phys. Rev. Lett. **71**, 3051 (1993), Astrophys. J. **460**, L25 (1996).

66. M. Bershady *et al.*, Phys. Rev. Lett. **66**, 1398 (1991);
M. Ressell, Phys. Rev. **D44**, 3001 (1991).

67. D. Grin *et al.*, Phys. Rev. **D75**, 105018 (2007).

68. B.D. Blout *et al.*, Astrophys. J. **546**, 825 (2001).

69. P. Sikivie, Phys. Rev. **D32**, 2988 (1985);
L. Krauss *et al.*, Phys. Rev. Lett. **55**, 1797 (1985);
R. Bradley *et al.*, Rev. Mod. Phys. **75**, 777 (2003).

70. P. Sikivie and J. Ipser, Phys. Lett. **B291**, 288 (1992);
P. Sikivie *et al.*, Phys. Rev. Lett. **75**, 2911 (1995).

71. S. DePanfilis *et al.*, Phys. Rev. Lett. **59**, 839 (1987);
W. Wuensch *et al.*, Phys. Rev. **D40**, 3153 (1989);
C. Hagmann *et al.*, Phys. Rev. **D42**, 1297 (1990).

72. S. Asztalos *et al.*, Phys. Rev. **D69**, 011101 (2004).

73. L. Duffy *et al.*, Phys. Rev. Lett. **95**, 091304 (2005).

74. S. J. Asztalos *et al.* (ADMX Collab.), arXiv:0910.5914.

75. M. Mück, J.B. Kycia, and J. Clarke, Appl. Phys. Lett. **78**, 967 (2001).

76. I. Ogawa, S. Matsuki, and K. Yamamoto, Phys. Rev. **D53**, 1740 (1996).

77. S. Matsuki *et al.*, Nucl. Phys. B (Proc. Suppl.) **51**, 213 (1996);
Y. Kishimoto *et al.*, Phys. Lett. **A303**, 279 (2002);
M. Tada *et al.*, Phys. Lett. **A303**, 285 (2002).